




The binding mode of pyrazolone derived copper(II), cobalt(II), nickel(II) and zinc(II) Schiff base coordination compounds with Calf-Thymus DNA

R.Paulpandiyan and N.Raman*

Research Department of Chemistry, VHNSN College (Autonomous), Virudhunagar-626 001

E-mail: ramchem1964@gmail.com

Abstract

Transition metal complexes with Schiff base ligands possess remarkable biomedical activities that could be used to develop new metal-based anticancer agents. Anticancer metal complexes have attracted considerable interest since the successful application of platinum based anti-cancer drugs. Pyrazolone derivatives have been extensively studied and have shown a wide range of pharmacological activities and anticancer activities. A new class of mononuclear copper (II), cobalt(II), nickel(II) and zinc(II) complexes were synthesized using pyrazolone precursor Schiff base, obtained by the condensation of 4-aminoantipyrine with salicylaldehyde and respective metal(II) chloride. They have been characterized by elemental analysis, magnetic susceptibility, molar conductance measurements, UV-Vis., FT-IR, ^1H NMR spectra and EPR studies. Their magnetic susceptibility values of the complexes at room temperature are consistent with octahedral geometry around the central metal ions. These complexes show lower conductance values, supporting their non-electrolytic nature. The data show that the complexes have composition of $[\text{ML}_2]$ type. *In vitro* DNA binding profiles of all complexes have been explored by absorption titrations, cyclic voltammetry technique and viscosity measurements. The corroborative results of above experiments suggest that these complexes are efficient metallo intercalators and can interact with CT-DNA. The binding constant values (K_b) clearly signify that the complexes bind to DNA through intercalation mode. The binding affinity of these complexes with CT DNA is found to be in the order, $\text{Cu(II)} > \text{Zn(II)} > \text{Co(II)} > \text{Ni(II)}$, among them copper complex displaying a higher binding propensity as compared to other complexes.

Keywords: Pyrazolone derivatives, octahedral geometry, non-electrolytic nature, intercalation mode

1. Introduction

Schiff bases are important intermediates for the synthesis of some bioactive compounds [1]. Furthermore, they are reported to show a variety of interesting biological actions [2]. Metal complexes of the Schiff base ligands have a variety of applications including clinical, analytical, biological, and organic synthesis [3-5]. Recent years have witnessed a great interest in the synthesis and characterization of transition metal chelates of pyrazolone derivatives. Among the pyrazolone

derivatives, 4-aminoantipyrine forms a variety of Schiff bases with aldehydes/ketones and is reported to be the superior reagents in biological, pharmacological, clinical and analytical applications [6]. A careful literature survey indicates that very little is known on transition metal complexes of Schiff bases having a pyrazolone ring. In this paper we report the synthesis, characterization, DNA binding studies of some transition metal complexes containing Schiff base derived from 4-aminoantipyrine and salicyl

aldehyde, with a special impetus on ligand structural investigations.

2. Experimental

The chemicals involved in this work were of AnalaR grade and were used without further purification. However, the solvents were purified by the standard procedure. 4-aminoantipyrine and salicylaldehyde were obtained from Sigma Aldrich. Solvents dimethyl formamide and dimethyl sulfoxide were procured from Himedia chemicals. All the metal salts were received from E-Merck. Elemental analysis (C, H and N) data were obtained using a Perkin-Elmer 240 elemental analyzer. Electronic spectra of the complexes were recorded on a Shimadzu Model 1601 UV-Visible Spectrophotometer in the wavelength range of 200-1100 nm. Vibrational spectra were performed on FT IR-Shimadzu model IR-Affinity-1 Spectrophotometer using KBr discs. The room temperature molar conductivity of the complexes in DMSO solution (10^{-3} M) was measured using a deep vision 601 model digital conductometer. The X-band EPR spectrum was performed at LNT (77 K). DNA binding experiments which include electronic absorption titration, viscosity and electrochemical methods conformed to the standard methods and practices previously adopted by our laboratory [7].

2.1 Synthesis

2.1.1 Synthesis of Schiff base ligand (HL)

The Schiff base ligand (salicylidene-4-aminoantipyrine) was prepared upon modification of the procedure reported by Raman et al [8].

2.1.2 Synthesis of Schiff base metal (II) complexes

The complexes were prepared by mixing the appropriate molar quantity of ligand and the corresponding metal salts using the following procedure. A solution of metal(II) chloride ($M = \text{Cu, Co, Ni and Zn}$)

in ethanol (2 mmol) was stirred with an ethanolic solution of salicylidene-4-aminoantipyrine (HL)(4 mmol), 1:2 molar ratio for 30 min on a magnetic stirrer at room temperature and it was refluxed for ca 3 h. Then the mixture was reduced to one-third on a water bath and cooled. The solid product formed was filtered and then recrystallized from ethanol and dried in *vacuo*.

3. Results and discussion

All the compounds are air stable for extended periods and the complexes are remarkably soluble in DMF and DMSO. The obtained elemental analysis data of the complexes are well comparable with the calculated values and show that the complexes may have the stoichiometry of $[\text{ML}_2]$. The lower molar conductance values ($10\text{-}18 \text{ ohm}^{-1} \text{ cm}^2 \text{ mol}^{-1}$) of the complexes support their non-electrolytic nature of the compounds. The proposed molecular structure of the Schiff base complex is depicted in Fig.1.

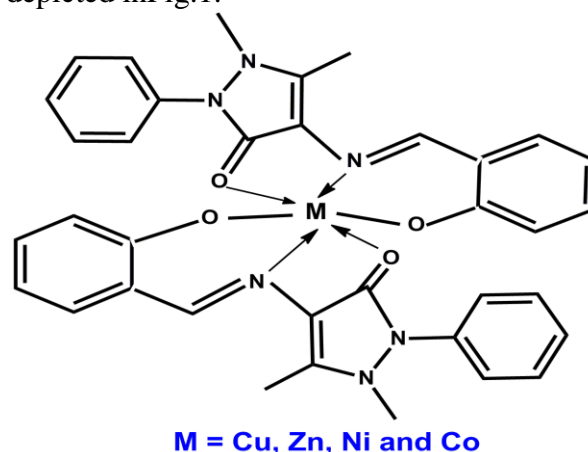


Fig.1 Proposed structure of the Schiff base complex

3.1 FT-IR spectroscopy

Comparisons of IR spectra of Schiff base ligand with that of its metal complexes have been adopted to determine the coordinating atoms of the ligand to metal ion. The IR spectrum of the ligand (HL) shows a weak broad band in the region

3000-3200 cm^{-1} allocated to intra-molecular hydrogen bonded -OH group. The absence of this band, noted in the spectra of the complexes, indicates the deprotonation of the -OH group on complexation. The -C=N bands of salicylidene-4-aminoantipyrine moiety appearing in the region 1610-1600 cm^{-1} for the free ligand are also shifted to lower frequencies in the spectra of the complexes (1580-1560 cm^{-1}) on coordination [7]. Coupled with this, HL also reveals a band at 1674 cm^{-1} allocated to ν (C=O) stretching mode which is shifted to lower frequency around 1645-1664 cm^{-1} indicating the coordination of the carbonyl oxygen atom of the ligand to metal ion. The coordination of the azomethine nitrogen and carbonyl oxygen was further supported by the appearance of new bands around 505-515 cm^{-1} and 452-464 cm^{-1} which are due to ν (M-O) and ν (M-N) respectively.

3.2 Electronic spectra and magnetic moments

The electronic spectra can often provide quick and reliable information about the ligand arrangement in metal complexes and also employ as a useful tool to predict geometries of the complexes. HL exhibits two intense bands in 35,154 and 29,658 cm^{-1} which are assigned to $\pi \rightarrow \pi^*$ and $n \rightarrow \pi^*$ transitions, respectively. In case of metal complexes, these transitions are shifted to longer wavelength due to the coordination of the ligand with metal ions. The electronic spectrum of Cu(II) complex displayed a d-d transition band at 14,136 cm^{-1} which can be assigned to ${}^2E_g \rightarrow {}^2T_{2g}$ transition, characteristic of d^9 distorted octahedral geometry [9]. The observed magnetic moment of the Cu(II) complex (1.82 BM) at room temperature specifies the non-coupled mononuclear complexes of magnetically diluted d^9 system with $s = 1/2$ spin state of distorted octahedral geometry. In Co(II) complex, this d-d band emerges at

13,456 cm^{-1} because of ${}^4T_{1g}(F) \rightarrow {}^4T_{2g}(F)$ transition which can be the evidence for octahedral geometry of d^7 Co(II) system. The observed magnetic moment value of this complex (2.75 BM) indicates the presence of three unpaired electrons, which suggests an octahedral geometry. The Ni(II) complex reveals d-d bands at 12,826 cm^{-1} , assigned to ${}^3A_{2g}(F) \rightarrow {}^3T_{1g}(F)$ transition. The examined magnetic moment value of this complex (3.35 BM) indicates the presence of two unpaired electrons and octahedral geometry is assigned. In contrast, Zn(II) complex does not exhibit any d-d band because of their completely filled d^{10} configuration.

3.3 EPR spectra

The EPR spectra of Cu(II) complex exhibit parameters like axially symmetric g-tensor with $g_{\parallel} (2.12) > g_{\perp} (2.06) > g_e (2.0023)$; $A_{\parallel} (140) > A_{\perp} (85)$ indicating that the copper site possesses $d_{x^2-y^2}$ ground state, characteristic of an octahedral geometry [10]. The geometric parameter G refers to a measure of the exchange interaction among the multiple copper centers in the polycrystalline compound. It is calculated by the following equation:

$$G = (g_{\parallel} - 2) / (g_{\perp} - 2)$$

As per earlier report, if value of $G > 4.0$, the local tetragonal axes exist in parallel alignment or slightly misaligned. In case value of $G < 4.0$, significant exchange coupling occurs and there is significant deviation. While the observed values for the exchange interaction parameter of Cu(II) complex fall within the range of 4.8 G, it suggests the local tetragonal axes are aligned in parallel or slightly deviated and the unpaired electron occupies in the $d_{x^2-y^2}$ orbital. At this state, it infers the absence of exchange coupling among the Cu(II) center in solid state [11].

3.4 ^1H NMR spectra

The NMR technique is highly useful to predict the structure of the compounds. The ^1H NMR spectra of the ligand and its Zn(II) complex were recorded in DMSO- d_6 . The spectrum of the ligand shows the following signals: C_6H_5 as a multiplet around the region 7.2-7.8 δ , $=\text{C}-\text{CH}_3$ at 2.7 δ and $-\text{N}-\text{CH}_3$ at 3.2 δ . The peaks at 11.2 δ attributed to the phenolic $-\text{OH}$ group present in the salicylaldehyde moiety. This peak is absent in the Zn(II) complex which confirms the loss of $-\text{OH}$ protons due to complexation. The azomethine proton appearing peak at 8.8 δ in free ligand is shifted to upfield region, supporting the coordination of $(-\text{HC}=\text{N})$ group to the metal center. There is no much difference in other signals of the complex.

3.5 DNA Binding Studies

3.5.1 Absorption Spectral Titrations

The change in the absorbance and shift in the wavelength at UV-visible region due to the addition of calf thymus DNA (CT DNA) to metal complex solution indicates the nature of interaction of the complexes with DNA. Thus the absorption spectra of these complexes in the absence or presence of CT DNA at different concentrations were measured. "Hyperchromic effect" and "hypochromic effect" are two types of spectral features of DNA, concerning its double-helix structure. This effect of spectral feature reveals the respective alternation of DNA in its conformation and structure while the drug binds to DNA. Hypochromism results from the contraction of DNA in the helix axis, as well as from the change in conformation on DNA, while hyperchromism results from the damage of the DNA doublehelix structure [30]. With the increase of [DNA], the absorption intensity of the complex decreases (hypochromic effect) and the λ_{max} values shift to red region (bathochromic shift) [12]. This occurs while

the binding induces a strong stacking interaction between the planar aromatic chromophoric groups of the ligand with DNA base pairs.

The absorption spectra of all the complexes showed an intensive absorption band in the region 270-384 nm, in 5 mM Tris-HCl/50 mM NaCl (pH 7.2) buffer solution. The observed hypochromicity values and their red shifts in the presence of DNA were observed in the region 1-3 nm which indicates the binding of DNA with the complexes is through intercalative mode [13]. The absorption spectra of the complexes (1) and (4) in the absence and presence of CT DNA in the UV region are depicted in Fig.2.

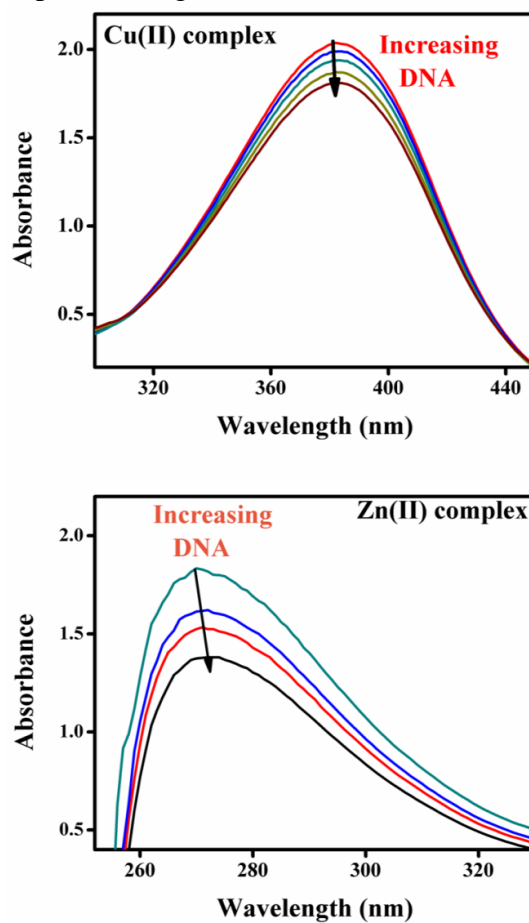


Fig.2 The absorption spectra of the complexes (1) and (4) in buffer pH =7.2 at 25 $^{\circ}$ C in presence of increasing amount of

CT DNA. Arrow indicates the changes in absorbance upon increasing the DNA concentration.

The intrinsic binding constant K_b values calculated from the slope to the intercept ratio from the plots between $[DNA]/(\epsilon_b - \epsilon_f)$ and $[DNA]$ are given in Table 1 and used to gather the information concerning the binding affinity of the complexes with CT-DNA. The binding strength of the complexes is shown as in the following order: **1>4>3>2**. Complex **1** reveals strong hypo chromism and a slight red shift as compared to other complexes highlighting its higher DNA binding propensity. These results imply that the intercalative ligands with extended aromatic plane and good conjugation effect can greatly support the DNA binding facility. The determined intrinsic binding constants for all the complexes are recline within the range $1.2-6.3 \times 10^4 \text{ M}^{-1}$. Comparing the values of K_b of the metal complexes with the classical intercalators, these complexes have lesser binding affinity than the classical intercalators such as EB [14] and higher than those of some Schiff base metal complexes [15] indicating that the present complexes strongly bind with DNA through an intercalation mode into the double helix structure of DNA.

Complex	$\lambda \text{ max}$		$\Delta\lambda$ (nm)	$K_b \times 10^4$ (M^{-1})
	Free	Bound		
[CuL ₂] (1)	381	384	3	6.3
[CoL ₂] (2)	338	340	2	3.6
[NiL ₂] (3)	336	339	3	1.2
[ZnL ₂] (4)	270	271	1	4.3

Table 1. Electronic absorption parameters for the interaction of CT DNA with synthesized complexes (1-4).

3.5.2 Viscosity Measurements

In order to verify the binding mode of complexes with CT-DNA, the DNA viscosity change at room temperature was measured by variable concentration of complexes. A classical intercalator EB shows a significant increase in relative viscosity of the DNA solution on intercalation due to an increase in overall DNA contour length on binding to DNA [16]. In contrast, partial or non-classical intercalation of complex would bend or kink the DNA helix, shortening the effective length of the DNA, and reducing DNA viscosity accordingly, while the electrostatic and groove binding cause little or no effect on the relative viscosity of DNA solution [17].

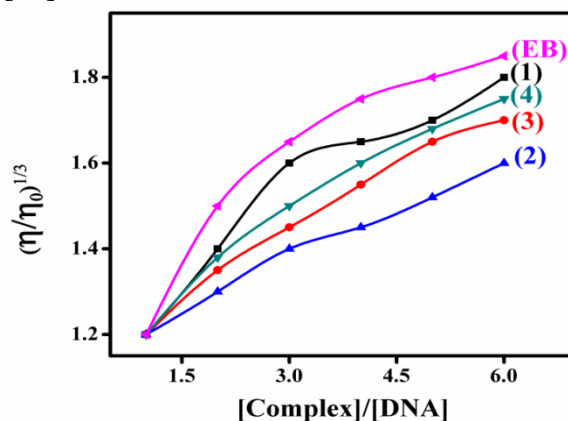


Fig.3. Effect of increasing amounts of [EB] and complexes (1-4) on the relative viscosity of CT DNA

The effects of all the synthesized complexes on the viscosity of DNA at $30 \pm 0.1^\circ\text{C}$ are shown in Fig.3. Viscosity measurements results clearly show that all the complexes can intercalate between adjacent DNA base pairs, causing an extension in the helix thereby increasing the viscosity of DNA. When the concentration of the complexes is increased, the complexes can intercalate strongly, leading to a greater increase in viscosity of the DNA. Hence, based on spectroscopic studies

Complex	$E_{1/2}(V)$	$\Delta E_p(V)$	I_p_a/I_p_c
	Free Bound	Free Bound	
[CuL ₂] (1)	-0.365 - 0.165	0.458 1.148	0.91
[CoL ₂] (2)	-0.465 - 0.205	1.258 2.148	0.84
[NiL ₂] (3)	-0.552 0.322	1.146 2.268	0.88
[ZnL ₂] (4)	0.567 0.652	2.301 2.402	0.94

Table 2. Electrochemical parameters for the interaction of CT DNA with synthesized metal complexes (1-4).

along with viscosity measurements, we can conclude that all these complexes interact with the DNA through an intercalation mode.

3.5.3 Electrochemical Behaviour

The electrochemical method is an important tool in examining the type and approach of DNA binding with metal complexes. Cyclic voltammetry has been chosen to understand the electrochemical properties of the complexes. Cyclic voltammetric studies of the complexes have been conducted in DMSO (10^{-3} M) at sweep rate of 0.5 V/s in the potential range, +2 to -2V. The characteristic cyclic voltammogram of the complexes 1 and 2 are depicted in Fig.4. The quasi-reversible redox couple for each complex has been analyzed upon the addition of CT DNA and shifts of $E_{1/2}$ and the ΔE_p is entered in Table 2. The incremental addition of CT DNA leads to substantial drop in the voltammetric current of the redox wave with a slight shift in $E_{1/2}$ to positive potential. The drop in current intensity can be elucidated in terms of an equilibrium mixture of free and DNA-bound complexes to the electrode surface [18]. This condition reveals that the complex stabilizes the duplex (GC pairs) by an intercalating mode. Evidently, the decline of the voltammetric currents in the presence of

DNA may be account table for the hindered diffusion of the metal complex bound to CT DNA. Both cathodic and anodic peaks show positive shift, which specifies the intercalation of complex to DNA base pairs [19].

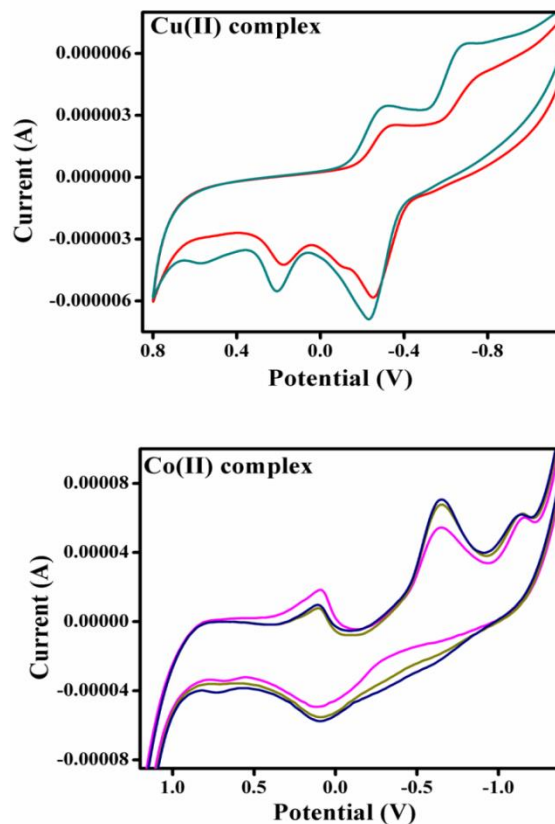


Fig.4 The cyclic voltammograms of the complexes 1 and 2 in buffer (pH = 7.2) at 25°C in presence of increasing amount of CT DNA.

Conclusion

Synthesis and characterization of a new set of pyrazolone precursor Schiff base and a series of transition metal (II) complexes of Cu, Zn, Co and Ni are reported as potential candidates to study their DNA binding effects. The physicochemical and spectral data infer that all these coordination compounds (1-4) exist as mononuclear and adopted octahedral

geometry around the metal center. DNA binding properties of all the above complexes were studied by electronic absorption spectra, cyclic voltammetry and viscosity measurement, which deduce their association as intercalative DNA interaction with different binding affinities. The binding strength of these complexes with DNA varies by the following order, **1>4>3>2**.

Acknowledgments

The authors express their heartfelt thanks to the College Managing Board, Principal and Head of the Department of Chemistry, VHNSN College (Autonomous), Virudhunagar for providing necessary research facilities. IIT Bombay (SAIF) and IIT Chennai, India are gratefully acknowledged for providing instrumental facilities.

References

1. A.E. Taggi, A.M. Hafez, H. Wack, B. Young, D. Ferraris and T. Lectka, *J. Am. Chem. Soc.* **124** (2002) 6626.
2. S.B. Desai, P.B. Desai and K.R. Desai, *Heterocycl. Commun.* **7** (2001) 83.
3. M. Usharani, E. Alila and R. Rajavel, *J. Chem. Pharmaceut. Res.*, **4**(1)(2012) 726.
4. A. Al-Amiery, A. A. H. Kadhum and A. B. Mohamad, *Bioinorg. Chem. Appl.*, **2012** (2012) 1.
5. B. Anupama and C. G. Kumari, *Res. J. Pharmaceut. Biolog. Chem.*, **2**, (2011) 140.
6. N. Raman, S. Sobha and A. Thamarachelvan, *Spectrochim. Acta A*, **78**(2011) 88.
7. R. Paulpandiyan and N. Raman, *Appl. Organomet. Chem.* **30**(2016) 531.
8. N. Raman, J.D. Raja and A. Sakthivel, *Russ. J. Coord. Chem.*, **34** (2008) 400.
9. Y. Prashanthi, K. Kiranmai, N.J.P. Subhashini and P. Shivaraj, *Spectrochim. Acta, Part A*, **70** (2008) 30.
10. G. Speier, J. Csihony, A.M. Whalen, and C.G. Pierpont, *Inorg. Chem.*, **35** (1996) 3519.
11. R.J. Dudleyand, and B. Hathaway, *J. Chem. Soc. A.* **12** (1970) 2794.
12. H. Chao, W.J. Mei, Q.W. Huang and L.N. Ji, *J. Inorg. Biochem.* **92** (2002) 165.
13. S. Zhang and J. Zhou, *J. Coord. Chem.* **61** (2008) 2488.
14. M.J. Waring, *J. Mol. Biol.* **13** (1965) 269.
15. T. Kiran, V.G. Prasanth, M.M. Balamurali, C.S. Vasavi, P. Munusamy and M. Pathak, *Inorg. Chim. Acta* **433** (2015) 26.
16. G.L. Eichhorn, and A. Shin, *J. Am. Chem. Soc.* **90** (1968) 7323.
17. B.D. Wang, Z.Y. Yang, P. Crewdson and D.Q. Wang, *J. Inorg. Biochem.* **101** (2007) 1492.
18. S. Tabassum, S. Parveen and F. Arjmand, *Acta Biomater.* **1** (2005) 677.
19. L.Z. Li, C. Zhao, T. Xu, H.W. Ji, Y.H. Yu, G.Q. Guo and H. Chao, *J. Inorg. Biochem.* **99** (2005) 1076.